Deep Learning Applications on Multitemporal SAR (Sentinel-1) Image Classification Using Confined Labeled Data: The Case of Detecting Rice Paddy in South Korea

Hyun-Woo Jo, Sujong Lee, Eunbeen Park, Chul-Hee Lim, Cholho Song, Halim Lee, Youngjin Ko, Sungeun Cha, Hoonjoo Yoon, and Woo-Kyun Lee

***Abstract*— The applicability of deep learning to remote sensing is rapidly increasing in accordance with the improvement in spatiotemporal resolution of satellite images. However, unlike satellite images acquired in near-real-time over wide areas, there are limited amount of labeled data used for model training. In this article, three kinds of deep learning applications—data augmentation, semisupervised classification, and domain-adapted architecture—were tested in an effort to overcome the limitation of insufficient labeled data. Among the diverse tasks that can be used for classification, rice paddy detection in South Korea was performed for its ability to fully utilize the advantages of deep learning and high spatiotemporal image resolution. In the process of designing each application, the domain knowledge of remote sensing and rice phenology was integrated. Then, all possible combinations of the three applications were examined and evaluated with pixel-based comparisons in various environments and city-level comparisons using national statistics. The results of this article indicated that all combinations of the applications can contribute to increase classification performance, even though the uncertainty involved in imitating or utilizing unlabeled data remains. As the effectiveness of the proposed applications was experimentally confirmed, enhancement in the applicability of deep learning was expected in various remote sensing areas. In particular, the proposed applications would be significant when they are applied to a wide range of study areas and high-resolution images, as they tend to require a large amount of learning data from diverse environments, owing to high intraclass heterogeneity.**

***Index Terms*— Data augmentation, data labeling, deep learning, domain adaptation, remote sensing, semisupervised classification.**

Manuscript received August 7, 2019; revised February 12, 2020; accepted March 9, 2020. Date of publication April 10, 2020; date of current version October 27, 2020. This work was supported in part by the International Research and Development Program of the National Research Foundation of Korea (NRF) through the Ministry of Science, ICT, and Future Planning under Grant 2018K1A3A7A03089842, in part by Korea University Grant, and in part by the European Commission under Contract H2020-776019 EOPEN. *(Corresponding author: Woo-Kyun Lee.)*

Hyun-Woo Jo, Sujong Lee, Eunbeen Park, Halim Lee, Youngjin Ko, Sungeun Cha, and Woo-Kyun Lee are with the Department of Environmental Science and Ecological Engineering, Korea University, Seoul 02841, South Korea (e-mail: leewk@korea.ac.kr).

Chul-Hee Lim is with the Institute of Life Science and Natural Resources, Korea University, Seoul 02841, South Korea.

Cholho Song is with the OJeong Eco-Resilience Institute (OJERI), Korea University, Seoul 02841, South Korea.

Honjoo Yoon is with Sundosoft Ltd., Seoul 08503, South Korea.

Color versions of one or more of the figures in this article are available online at http://ieeexplore.ieee.org.

Digital Object Identifier 10.1109/TGRS.2020.2981671

I. Introduction

With the advancement in satellite technology, the increased spatiotemporal resolution of satellite images is accelerating remote sensing data to become big data [1]. As properties of data are transformed, analytical methods are also evolving [2], [3], and the massive volume and complexity of satellite images are increasing the applicability of deep learning in the remote sensing field. However, because of the nature of deep learning analysis, which requires vast amounts of training data for desirable performance, the lack of labeled data is a prevalent problem in deep learning studies [4]. In particular, the imbalance between labeled and unlabeled data is extreme in remote sensing, which provides near-real-time images over wide areas [5]. Therefore, to promote the applicability of deep learning in remote sensing, techniques to overcome overfitting on the traits of a confined labeled area should be developed based on target domain knowledge and data science approaches.

Among the various classification tasks, the detection of rice paddy in South Korea, a representative task that is limited in classical remote sensing analysis, was the focus of this article. Because many rice paddies in South Korea are fragmented, as in many Asian countries, reflectance from other objects may be diluted to the adjacent rice paddy when observed by midlow resolution satellite imaging [6]. Given that the state-of-the-art satellites provide more precise observation of fragmented rice paddies, with high spatiotemporal resolution, and that the ability of deep learning to simulate both nonlinear and autoregressive phenomenon is effective for modeling phenological changes in vegetation [7], the detection of rice paddy was considered an optimal task for examining diverse deep learning applications.

Several deep learning models had already been applied to land cover classification and crop mapping in previous studies, including rice paddy detection [8], [9]. They experimentally demonstrated the applicability of deep learning to remote

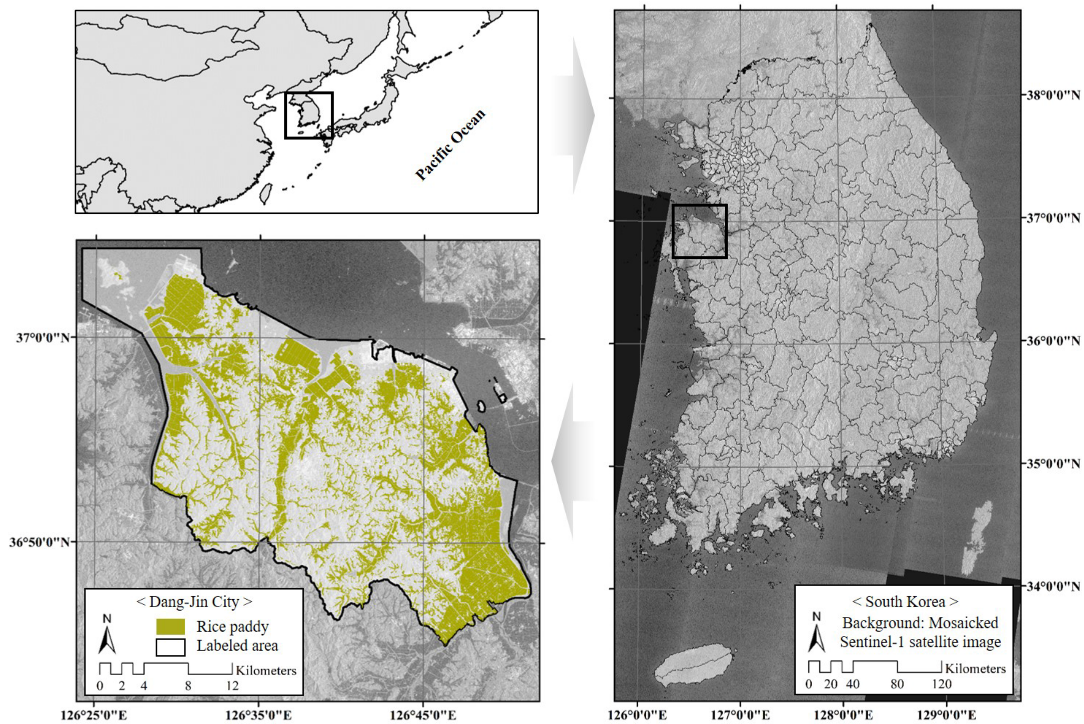

Fig. 1. Confined labeled data in Dangjin city, South Korea.

sensing and its comparative advantages over classical machine learning. However, these studies did not focus on overcoming the limitation of insufficient labeled data nor did they adapt domain knowledge of the target objects in the design of deep learning architecture, while using generally known architectures. Rather, studies using classical machine learning, in which most of the feature extraction processes rely on researchers, tend to adapt domain knowledge sufficiently in the classification model. For example, by considering phenological patterns into rice paddy detection [10], which most of deep learning researches have neglected, classical machine learning could improve its performance. Therefore, even as deep learning performs end-to-end learning, which automatically extracts features, it also needs to adapt domain knowledge in the architecture design process to maximize classification performance and overcome the limitation of sparse labeled data [11].

In this article, diverse applications, such as data augmentation, semi-supervised classification, and domain-adapted architecture, were examined in the deep learning-based rice paddy detection model to overcome the limitation of labeled data established in a confined area. Each application is designed to adapt domain knowledge, such as rice planting season, and spatial information that appears in satellite imagery. The applications were implied to South Korea both independently and in combination. Based on the results, the effectiveness of the sets of applications was compared.

II. Materials

A. Study Area

In this article, rice paddy detection was conducted across all of South Korea by only using labeled data in a confined area (Fig. 1). Located in the midlatitude region, South Korea has a temperate monsoon climate with a humid summer and dry winter [12]. The average annual precipitation is approximately 1200 mm, with 50%–60% of precipitation concentrated in the rainy season from June to August. Most plains are located in the western part of the country, and the eastern part is mountainous. Rice farming is generally performed by transplanting in May–June and harvesting in September–October. In the case of early harvests, other crops could be cultivated on the harvested rice paddy; however, rice is mostly cultivated once a year.

B. Remote Sensing Data

In this article, diverse deep learning applications were examined with time series of Sentinel-1 satellite images as a major premise of this research is to utilize high spatio-temporal data set with massive volume and complexity. To detect fragmented rice paddies in Asia, satellite images with high spatial resolution are required [13]. At the same time, high temporal resolution is also required to reflect rice phenology on the classification model. Sentinel-1, launched by the European Space Agency in 2014 and 2016 for each twin satellite, provides 10-m resolution images with 6 days of revisit time. With its distinguished spatiotemporal resolution, Sentinel-1 also has the advantage of synthetic aperture radar (SAR), which collects data in all types of weather using a radar sensor. The multitemporal backscattering value, which is consistently observed with SAR, is known to be effective in monitoring the growing stage of rice, represented as a function of rice phenology [14]. Between VV and VH polarization, which Sentinel-1 provides, VH polarization was used in this article for its superiority over VV in overall land cover separability including rice paddy [15].

Time series of Sentinel-1 images were acquired through Google Earth Engine (GEE) to minimize time and labor spent on data preprocessing. The area of South Korea is 100 364 km^2, and the cost of collecting, integrating, processing, and storing a high-resolution time-series data set from such a large area can be significantly reduced by using web-based platforms such as GEE. To use an independent data set in the processes of model production and application, the 2017 images were used as training and validation data, whereas the 2018 images were used as test data. Sentinel-1 images from GEE were provided after a series of preprocessing tasks was performed, such as updating orbit metadata, ground range-detected (GRD) border noise removal, thermal noise removal, radiometric calibration, and terrain correction (https://developers.google.com/earth-engine/sentinel1). In the case of GRD border noise removal, preprocessing was not applied to the images taken before 2018. Therefore, additional borderline noise removal was performed by applying a minimum threshold value of −46 dB. The threshold was selected by acquiring a natural break point in the histogram between imagery and noise in the yearly minimum-value composite image. Then, 46 dB was added to the entire image for calculating the Paddy rice Mapping Index (PMI), which will be dealt with at latter part. The addition was intended to set image not to have negative values while maintaining data scale and histogram pattern.

C. Labeled Data

To avoid mislabeling high-resolution Sentinel-1 images, precise labeling data compatible to 10-m resolution should be acquired. Therefore, in this article, the parcel-level rice paddy area was extracted from the level-three land cover map, which has the highest resolution among three different scales of land cover maps produced by Korean Ministry of Environment. The minimum classification criteria of the level-three land cover map are 3-m wide for linear elements and 10 m × 10 m (100 m^2) for plane elements, which provide compatible or more detailed resolution compared with Sentinel-1. The land cover map is produced by an on-screen digitizing method using KOMPSAT-2 and IKONOS satellite images, orthorectified aerial photos, and an existing domestic GIS data set [16]. In addition, ambiguous areas that are not clearly classified in remote sensing data are investigated by field survey.

Although land cover maps of the entire nation are available, products for each region have been outdated for several years as a tradeoff with high quality. Therefore, the labeled data was confined to the area of Dangjin city, which is the greatest rice producer in South Korea (Fig. 1). The land cover map in Dangjin city was produced in 2015; thus, it was updated to the status of 2017, which is the period of the training and validation data set. The update was performed by visual interpretation using Google Earth Pro and domestic street view services (https://map.kakao.com; https://map.naver.com) with a cross-validation of three interpreters. In the process of the update, a small portion of the sea nearby was also labeled in addition to the administration area of Dangjin city to train water environments. After the update, it was converted into raster format with a resolution compatible with Sentinel-1. The labeled area in Dangjin consists of 7 458 996 pixels (745 km^2), among which 2 345 812 pixels (235 km^2) are of rice paddy.

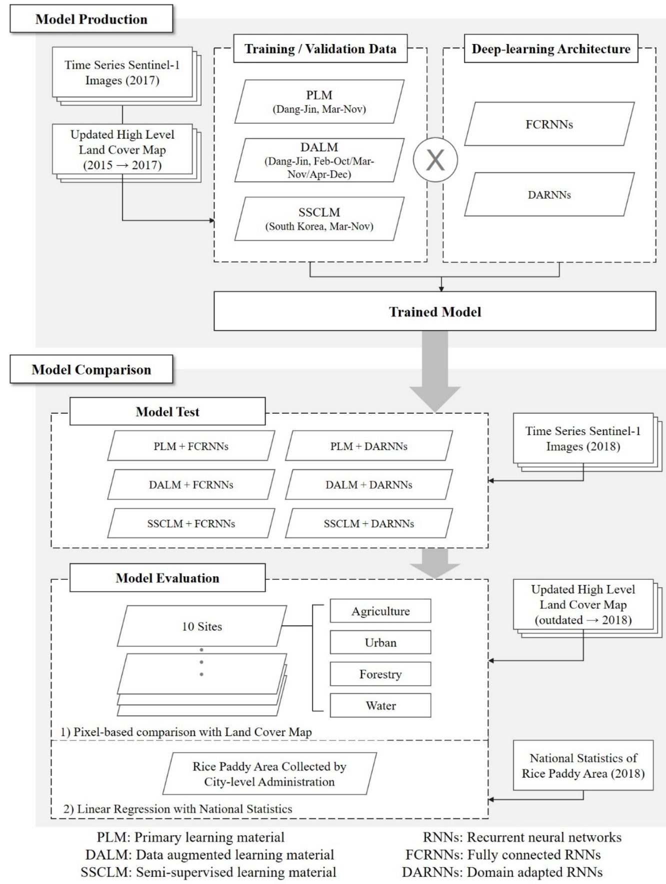

Fig. 2. Research flow for application examination.

III. METHODOLOGY

In this article, a number of deep learning applications are examined to maximize classification performance using remote sensing data with a confined labeled area. To compare performance, diverse sets of applications were implied based on a baseline application set that is composed of primary learning material (PLM), produced with the 2017 data in Dangjin city, and fully connected recurrent neural networks (FCRNNs) (Fig. 2). Data augmentation and semi-supervised classification were applied to PLM to derive data-augmented learning material (DALM) and semi-supervised classification learning material (SSCLM). Domain-adapted RNNs (DARNNs) is a modified architecture of FCRNNs that considers phenological differences of rice in South Korea. In summary, the concatenation of three learning materials and two deep learning architectures were examined. After the models were produced, they were tested over all of South Korea with the 2018 data. Then, two types of evaluation were performed: pixel-based comparison was conducted in ten sites using an updated land cover map, with each site consisting of four different types of landscapes—agricultural, urban, forestry, and water—and statistical evaluation was conducted by calculating

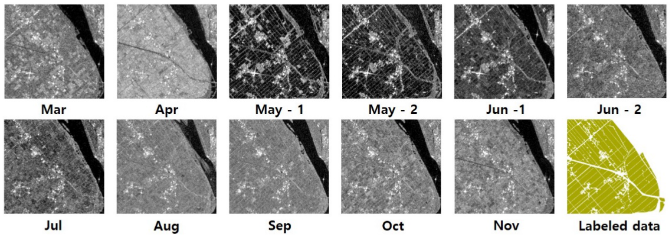

Fig. 3. PLM consisting of 11 time-series images and labeled data.

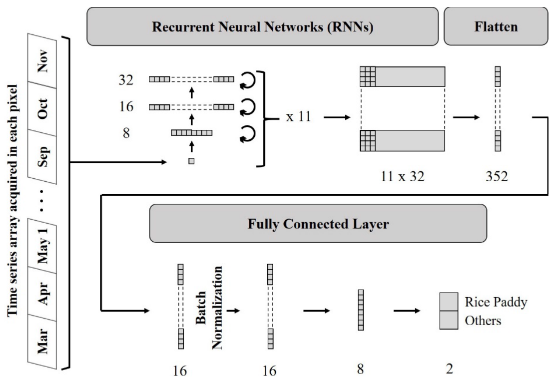

Fig. 4. FCRNN architecture.

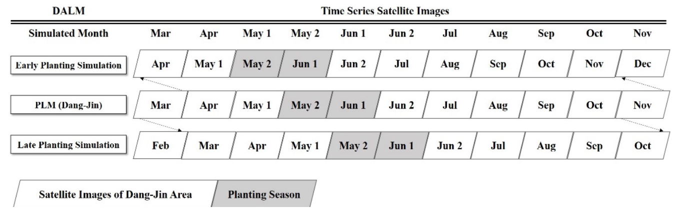

Fig. 5. DALM: Data augmented data set derived from PLM.

linear regression equation between the classification result and national statistics.

A. Baseline Application

The baseline application set is a combination of PLM and FCRNNs that serves as a control group to evaluate the sets of deep learning application. PLM was produced by stacking 11 time-series Sentinel-1 images and labeling it with the level-three land cover map of Dangjin in 2017 (Fig. 3). Each image is a monthly mean value composite from March to November, except May and June, which are mean-value composites of a half-month. May and June have a more frequent observation interval because they are in the planting season of rice, which can serve as a significant feature to improve classification accuracy with a dramatic change in the backscattering value [17]. Because almost all rice paddies in South Korea are irrigated in the planting season, low backscattering values are recorded in the planting season, reflecting the smooth surface of water, and high backscattering values are recorded, reflecting the coarse surface of rice as the grain grows. There is an exception at rice paddies in which direct dry-seeding is conducted; however, the use of this method is declining, comprising less than 0.1% of the total rice paddy in 2016 [18]. The learning material was divided into 60% training area and 40% validation area through a random sampling method.

FCRNNs architecture is designed to extract high-level features from rice paddy monitoring data. The architecture consists of three RNN layers and four fully connected layers, with one batch normalization layer between them (Fig. 4). The RNN part was aimed to extract features from the autoregressive pattern of the backscattering values in the growing rice paddy. With a closed-loop structure, outputs of a particular time series in RNN layers are involved in the function of the next time-series data and effectively extract features from autoregressive time-series data [19]. The multiple, fully connected layers are aimed to extract high-level features that could perform noise-invariant classification through the application of highly nonlinear functions with deep architecture [20]. The batch normalization layer served to prevent the gradient vanishing problem that impedes model training, especially in deep architecture, and reduce overfitting on the limited labeled data [21].

B. Data Augmentation

Data augmentation techniques are used to acquire a large number of learning material by transforming data to the extent that they do not impair the intrinsic attributes of the classification target. Usually, image deformation, such as rotation, partitioning, scaling, and brightness adjustment, are mainly used for many studies [22]. However, the major differences between the learning area and the entire country could be explained through temporal differences rather than spatial differences from the perspective of rice detection. For example, the optimal rice planting season in South Korea varies from May 7 to June 21, depending on the latitudinal temperature gradient, topographical difference, and type of rice species such as early-, medium-, and late-maturing rice [23]. In addition, trends of backscattering value from planting to harvesting are very coincident even if diverse parcels have different sowing date [24], so a shift of time-series backscattering value could minimize the phenological differences in diverse regions. Therefore, this article tried to simulate the rice phenology that appears in the multitemporal images by considering the differences in the growing period depending on regional and species differences. In summary, data augmentation on the time dimension was applied to the PLM and produced DALM to simulate diverse rice phenology from the confined labeled area. In Dangjin, located on the central west coast, rice is planted from late May to early June, which is the middle of the national optimal planting period. Thus, the time-series data of the early- and late-planting areas were simulated by moving back and forth between the time-series satellite images of the Dangjin area (Fig. 5).

C. Semisupervised Classification

Semisupervised classification is a technique to exploit the unlabeled data on supervised learning by clustering data with unsupervised classification and labeling the clustered data

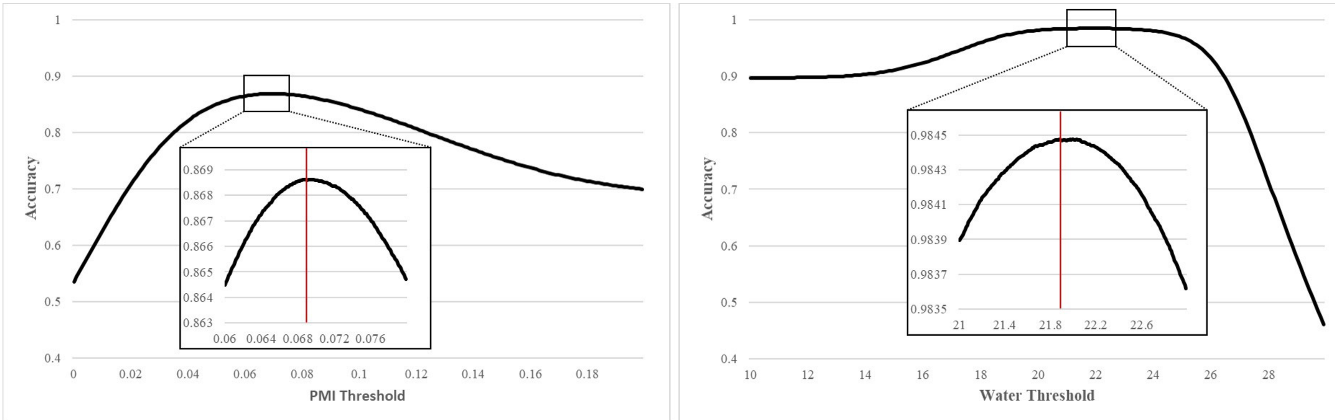

Fig. 6. PMI and water threshold selected in the Dangjin area.

thorough existing labeled data. In this article, SSCLM was produced by applying semisupervised classification to images of the entire country with reference to PLM. To fully utilize domain knowledge, object-based classification was applied to the unsupervised classification process. The concept of object-based classification considers not only the similarity of the multitemporal backscattering value but also the spatial adjacency [25], providing an additional dimension when clustering the spatial data. Object-based clustering was performed with a multiresolution segmentation algorithm in Definiens Developer software that produces small homogeneous clusters by locally minimizing the average heterogeneity [26]. The clustered objects were labeled with modified PMI classification, which is a supplemented version of the PMI-based classification introduced by Park *et al.* [27]. Modified PMI classification was developed to minimize misclassification between the rice paddy and river side plants by subtracting the flooded area from the assumed rice paddy area:

$$\begin{aligned}\text{Ricepaddy} = \{&\text{PMI,Water}|\text{PMI} > \text{PMI threshold},\\ &\text{Water}<\text{Water threshold}\}\end{aligned} \tag{1}$$

$$\text{PMI} = \frac{\text{SAR (Harvest)} - \text{SAR (Transplanting)}}{\text{SAR (Harvest)} + \text{SAR (Transplanting)}} \tag{2}$$

$$\text{Water} = \text{SAR (Rainyseason)} \tag{3}$$

where $\text{SAR}(x)$ indicates the mean value composite of the SAR images in period x.

A national timescale was considered for the selection of each time parameter—May–June for transplanting, July–August as the rainy season, and October–November for harvesting. A PMI threshold and water threshold of 0.0686 and 21.88, respectively, was selected to maximize the classification accuracy in the Dangjin area (Fig. 6).

D. Domain-Adapted Architecture

When acquiring sufficient learning materials is difficult, model performance can be alternatively improved by adapting domain knowledge in the process of model design [11]. In this article, the knowledge of differences in rice phenology, which were mentioned in the data augmentation application, was adapted on FCRNNs architecture to produce DARNNs. DARNNs are the architecture with 1-D convolution and max pooling layers added to the FCRNNs to extract features from the computation between adjacent time-series data. The architecture consists of two 1-D convolution layers, two RNN layers, one max pooling layer, and four fully connected layers with one batch normalization layer between them (Fig. 7). Unlike FCRNNs, two layers of 3 by 1 convolution filters were introduced to DARNNs, with the effect of reducing the temporal variability within the window size by applying it along the time axis [28]. The following max pooling layer after the RNN structure makes the feature extraction process invariant to a small time shift [28], [29]. Both types of additional layers are intended to increase the applicability of the model over diverse rice phenology.

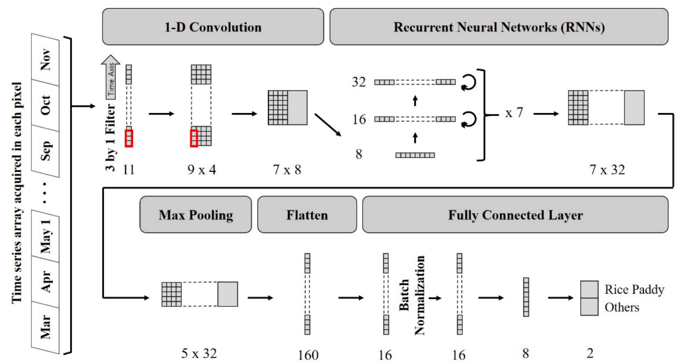

Fig. 7. Domain adapted RNN (DARNN) architecture.

E. Model Evaluation

Models were produced for the combination of each learning material and deep learning architecture; then, they were tested on the time-series images of 2018. For the classification results, postprocessing for noise reduction was performed with an adaptive filter that operates as follows.

Let rice paddy be 1 and others be 0:

$$i_{xy} = \begin{cases} 1, & \sum_{h=y-1}^{y+1} \sum_{w=x-1}^{x+1} i_{hw} \geq 4 \\ 0, & \sum_{h=y-1}^{y+1} \sum_{w=x-1}^{x+1} i_{hw} < 4 \end{cases} \tag{4}$$

TABLE I
RESULTS OF PIXEL-BASED EVALUATION

Model	Value Idx.		A	B	C	D	E	F	G	H	I	J	Total
PLM + FCRNNs	Plot Acc.	Agricultural	88.28	88.26	89.07	82.57	88.00	87.74	82.19	85.08	71.28	77.37	83.92
		Urban	99.57	99.68	100.00	96.15	96.38	94.22	91.02	98.86	99.92	98.80	97.45
		Forestry	100.00	99.99	100.00	99.00	99.90	99.73	99.50	99.87	99.82	99.97	99.77
		Water	99.98	99.99	99.84	99.98	99.84	87.72	97.77	100.00	99.78	100.00	98.48
	Sites Acc.		96.96	96.98	97.23	94.43	96.02	92.35	92.62	95.96	92.70	94.03	94.91
	Cohen's Kappa		0.81	0.67	0.76	0.70	0.88	0.79	0.70	0.87	0.67	0.78	0.79
DALM + FCRNNs	Plot Acc.	Agricultural	89.43	91.79	92.29	85.40	89.00	92.96	84.80	91.77	87.33	86.99	89.16
		Urban	99.57	99.80	100.00	96.78	97.79	95.53	93.26	98.80	99.86	98.84	98.02
		Forestry	100.00	99.98	100.00	99.19	99.91	99.80	99.46	99.82	99.74	99.85	99.77
		Water	99.97	99.97	99.90	99.93	99.92	91.21	99.35	100.00	97.00	99.97	98.72
	Sites Acc.		97.25	97.88	98.05	95.33	96.65	94.87	94.22	97.60	95.98	96.41	96.42
	Cohen's Kappa		0.82	0.77	0.84	0.76	0.90	0.86	0.77	0.93	0.85	0.88	0.86
SSCLM + FCRNNs	Plot Acc.	Agricultural	88.73	90.44	91.25	84.71	88.79	89.26	83.46	90.45	86.15	83.96	87.70
		Urban	99.58	98.37	99.99	95.63	97.29	95.00	91.58	99.07	99.94	99.15	97.56
		Forestry	100.00	100.00	100.00	99.54	99.93	99.80	99.48	99.93	99.98	99.99	99.87
		Water	100.00	99.99	99.99	100.00	99.96	90.53	96.45	100.00	99.00	99.98	98.58
	Sites Acc.		97.08	97.20	97.81	94.97	96.49	93.65	92.75	97.36	96.27	95.77	95.93
	Cohen's Kappa		0.80	0.70	0.81	0.73	0.90	0.83	0.70	0.92	0.86	0.85	0.83
PLM + DARNNs	Plot Acc.	Agricultural	88.10	90.19	89.40	84.92	88.37	89.55	81.67	88.74	81.02	75.92	85.74
		Urban	99.60	99.82	100.00	96.95	96.94	94.64	90.29	98.97	99.92	99.25	97.63
		Forestry	100.00	99.98	100.00	99.27	99.88	99.75	99.48	99.91	99.85	99.91	99.80
		Water	99.98	99.99	99.92	99.98	99.87	88.82	98.02	100.00	99.92	99.98	98.64
	Sites Acc.		96.92	97.50	97.33	95.28	96.26	93.19	92.37	96.91	95.18	93.76	95.45
	Cohen's Kappa		0.80	0.71	0.76	0.74	0.89	0.81	0.67	0.91	0.80	0.76	0.81
DALM + DARNNs	Plot Acc.	Agricultural	89.10	91.90	92.25	85.62	88.94	92.70	84.72	91.85	87.56	86.55	89.10
		Urban	99.59	99.80	100.00	96.55	97.75	95.48	93.14	98.90	99.90	98.88	97.99
		Forestry	99.99	99.99	100.00	99.21	99.93	99.78	99.43	99.85	99.75	99.85	99.78
		Water	99.97	99.98	99.92	99.94	99.93	91.09	99.14	100.00	98.03	99.98	98.79
	Sites Acc.		97.17	97.92	98.04	95.33	96.63	94.76	94.11	97.65	96.31	96.31	96.42
	Cohen's Kappa		0.81	0.77	0.84	0.76	0.90	0.86	0.76	0.93	0.86	0.87	0.86
SSCLM + DARNNs	Plot Acc.	Agricultural	88.73	90.53	91.17	84.81	88.78	89.56	83.27	90.42	85.99	83.58	87.66
		Urban	99.56	98.33	99.99	95.68	97.29	95.01	91.44	99.08	99.94	99.10	97.54
		Forestry	100.00	100.00	100.00	99.56	99.93	99.80	99.48	99.94	99.97	99.99	99.87
		Water	99.99	99.99	99.99	100.00	99.96	90.56	96.65	100.00	99.04	99.98	98.61
	Sites Acc.		97.08	97.21	97.79	95.01	96.49	93.73	92.71	97.36	96.24	95.66	95.92
	Cohen's Kappa		0.80	0.70	0.81	0.73	0.90	0.83	0.70	0.92	0.85	0.84	0.83

PLM: Primary learning material, DALM: Data-augmented learning material, SSCLM: Semi-supervised learning material, RNNs: Recurrent neural networks, FCRNNs: Fully connected RNNs, DARNNs: Domain-adapted RNNs.

where x and y are column- and row-wise coordinates each and i_{xy} indicates the classification result in pixel (x, y).

To evaluate model performance in diverse environment, ten evenly distributed evaluation sites were selected in South Korea, with each site consisting of four plots from agricultural, urban, forestry, and water landscapes. The size of each plot varies a little from 6 to 6.4 km^2, according to its location under the projection of the Korean Central Belt (EPSG: 5186), which consists of a GRS80 spheroid and Transverse Mercator projection with a central meridian of 127°. The evaluation plots were labeled by updating the level 3 land cover map to 2018, with the visual interpretation and cross-validation of three interpreters in the same method as that of labeling learning materials. With a pixel-based comparison, the classification accuracy was calculated for each site and plot, whereas Cohen's kappa value was calculated only for the sites. This is because plots other than the agricultural area have few or no rice paddies, causing difficulties in the interpretation, which results in inharmonicity between the low kappa value and high rate of concordance.

Furthermore, additional evaluation was performed by comparing the classification result with the national city-level statistics for the rice paddy area provided by Statistics Korea [30]. The statistical data is produced by a "crop production survey" on the basis of a field survey of 32 000 sample areas to confirm agricultural land use and 22 000 sample areas to confirm rice planting [31]. In the statistical evaluation, a linear regression was calculated between the statistics and the rice paddy area gathered from the pixels to the city boundaries. Among the 162 cities, 160 cities were compared, omitting Ulleung and Taean, since the former that consists of islands in the far East Sea with no rice paddy increased computational inefficiency and the latter contains parts with no imagery. At this step, the overall trend in model performance was identified, such as whether the result represented over- or underestimation.

IV. RESULTS AND DISCUSSION

A. Pixel-Based Model Comparison

Table I shows the pixel-based evaluation results of six models, composed of data augmentation, semisupervised classification, and domain-adapted architecture, for ten sites which of geographical information are introduced at Table II. To avoid the randomness of deep learning in the process of parameter initialization [32], the result on the table was selected from the median accuracy model for the seven times training was performed for each application set. The effect of randomness to the accuracy was not significant, as 0.003169 was recorded by averaging the accuracy variances of the seven training runs for each application set.

TABLE II
GEOGRAPHICAL INFORMATION OF EACH SITES AND PLOTS

Site	Plot	Lat.	Long.	Area (pixels, 100 m^2)
A	Agricultural	38.2625	128.5375	60,644
	Urban	38.2125	128.5875	60,782
	Forestry	38.2375	128.4625	60,774
	Water	38.2875	128.5625	60,734
B	Agricultural	37.9375	127.7625	61,002
	Urban	37.8625	127.7375	61,069
	Forestry	37.9125	127.8375	61,013
	Water	37.9375	127.8375	60,991
C	Agricultural	37.5625	126.7625	61,292
	Urban	37.5375	126.8375	61,339
	Forestry	37.6375	126.9875	61,217
	Water	37.5125	126.9875	61,438
D	Agricultural	36.9875	127.7625	61,783
	Urban	36.9625	127.9375	61,791
	Forestry	36.9375	127.8625	61,812
	Water	36.9375	128.0375	61,825
E	Agricultural	36.7875	126.8125	62,028
	Urban	36.8875	126.6375	61,842
	Forestry	36.7375	126.6125	61,951
	Water	36.9125	126.2625	61,833
F	Agricultural	36.3625	128.4375	62,261
	Urban	36.4125	128.1625	62,214
	Forestry	36.3875	128.5375	62,235
	Water	36.2875	128.3375	62,330
G	Agricultural	35.7125	128.0125	62,789
	Urban	35.6875	127.9125	62,762
	Forestry	35.5625	127.9875	62,860
	Water	35.5875	128.0375	62,870
H	Agricultural	35.6375	126.7375	62,764
	Urban	35.5625	126.8625	63,082
	Forestry	35.6125	126.5375	62,794
	Water	35.5625	126.5625	62,855
I	Agricultural	35.1875	128.8875	63,210
	Urban	35.2375	128.9125	63,178
	Forestry	35.2625	128.8875	63,156
	Water	35.0875	128.9375	63,292
J	Agricultural	34.5625	126.6625	63,648
	Urban	34.7625	126.4375	63,465
	Forestry	34.4625	126.6125	63,691
	Water	34.3875	126.4625	63,739

According to the result, the overall performance was best for the models of "DALM + DARNNs" and "DALM + FCRNNs," recording an accuracy of 96.42% and kappa value of 0.86. This was followed by "SSCLM + FCRNNs" and "SSCLM + DARNNs," recording similar accuracies of 95.93% and 95.92%, respectively, with the same kappa value of 0.83. In sequence, "PLM + DARNNs" recorded 95.45% accuracy and 0.81 kappa value, and "PLM + FCRNNs," a baseline application set, recorded the lowest performance with 94.91% accuracy and a kappa value of 0.79. Considering the margin of accuracy remaining up to 100% is less than 6%, an increase in accuracy of approximately 1% is very significant. In the same context, the general classification patterns are similar in most properly trained models as a great part of the image is in a clearly separable area. The value of a sophisticated model comes from classifying the obscure area accurately, and it is expressed as a small but consistent increase in accuracy. Given that the accuracy variance among the application sets is recorded as 0.3387 which is relatively huge compared with that of the repeated training in the same application, the effect of the applications is meaningful.

Although there are some variances from the models, in general, sites A, B, C, and H represented high performance compared with all models, as most of them recorded over 97% accuracy, whereas sites D, F, and G represented low performance with most of them recording under 95% accuracy or 0.80 kappa value. According to the landscape type in each plot, every model recorded a mean accuracy of over 97% for urban, forestry, and water, whereas the accuracy varies from approximately 83% to 90% for the agricultural landscape.

Fig. 8 shows the change in accuracy at each site comparing the application sets to the "PLM + FCRNNs," which is the baseline application set. In site E, which is adjacent to the labeled area in Dangjin, the effects of the applications were not significant. However, as the distance from the labeled area increases, the effects of the applications for improving accuracy tend to increase as well, which suggest that the use of domain-adapted applications is effective in improving classification performance, particularly in areas with different environmental conditions from a confined labeled area.

Therefore, the advantage of using such applications is maximized when the intraclass heterogeneity of the classification target is high, which usually occurs with a study area that has a wide range and high spatial resolution, with a pixel size smaller than the target objects [33]–[35]. In the meantime, with the advancement in information and communications technology and data processing techniques, analyzing high-resolution images over the large area is facilitated by the use of web-based platforms. Recently, platforms, such as opEn interOperable Platform for unified access and analysis of Earth observatioN data (EOPEN), are under development to enable deep learning analysis on such big and complex data (https://eopen-project.eu) [36]. The combination of the aforementioned applications and the platform is expected to promote the applicability of deep learning to remote sensing.

Comparing the effectiveness of each application through the evaluation indices, the data augmentation has the greatest effect on the performance improvement. Applying only data augmentation on the baseline application set, "DALM + FCRNNs" recorded the best performance. Semisupervised classification also improved the classification performance by improving the kappa value and more than 1% of accuracy from that of baseline application set in both models using SSCLM. In summary, it is experimentally found that classification performance is improved in order of DALM, SSCLM, and PLM when it comes to the use of learning materials. However, it should be noted that the degree of performance improvement may vary depending on how well the domain knowledge is adapted. In particular, the effect of semi-supervised classification varies significantly depending on the process of utilizing the unlabeled data [37].

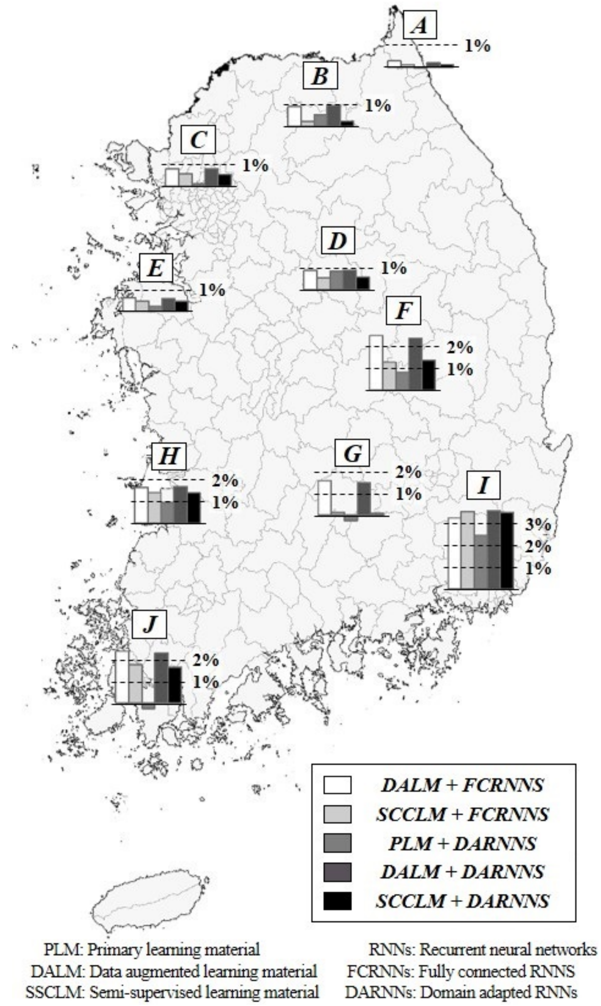

Fig. 8. Change in accuracy at each site compared to the baseline application.

Model performance was also improved when the domain knowledge was adapted to the process of deep learning architecture design. Improvement was observed when it was solely applied to the baseline application set with an accuracy improvement of 0.54%. However, the effect of domain-adapted architecture was hard to recognize when it was accompanied with data augmentation or semisupervised classification. There was no synergistic effect but rather only the recording of better performance of the application among the combination. It is assumed that the improvement in the performance was limited because the same type of domain knowledge has been considered in both simultaneously applied applications, which is the difference in rice phenology.

To identify the factors affecting classification performance, the rice paddy detection patterns on agricultural plots were analyzed. The biggest differences identified by visual analysis on site A and G, which are the typical high- and

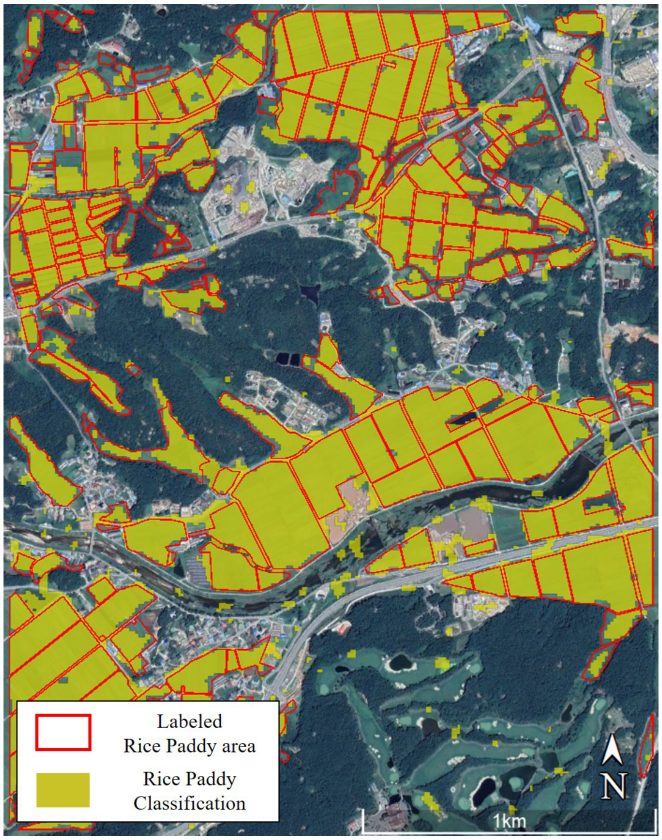

(a)

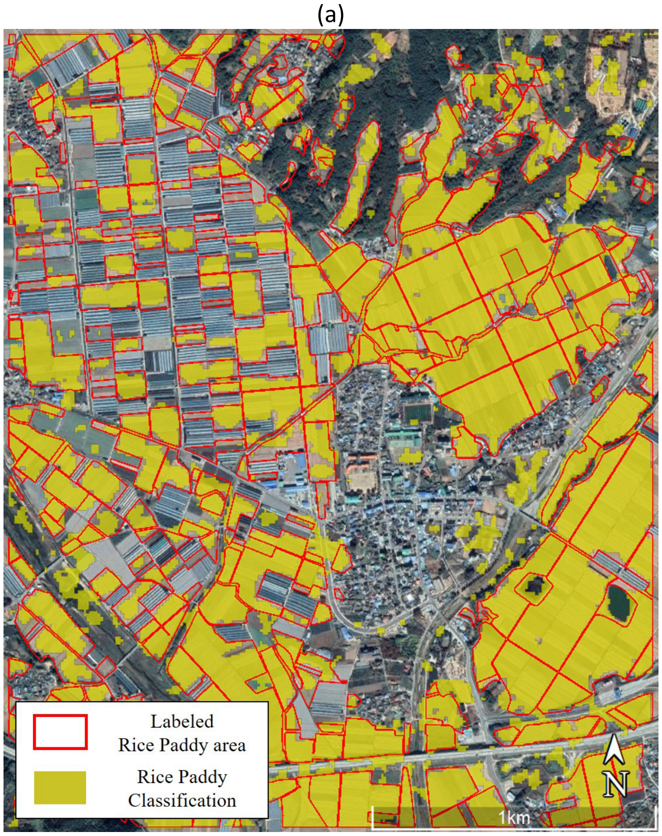

(b)

Fig. 9. Rice paddy detection results of "PLM + DARNNs" in agricultural plots at (a) sites A and (b) site G.

low-performance areas, were the degree of rice paddy fragmentation and the presence of artificial structures adjacent to the paddies. Whereas, the agricultural plot of site A consists of large patches, that of site G consists of a number of small fragmented patches with agricultural facilities nearby (Fig. 9).

According to the analysis, the types most commonly misclassified were small objects below the resolution of satellite images, radar shadows due to artificial structures, and river side plants that shows similar phenological patterns to rice paddies (Fig. 10). Whereas the first two types are caused by the limitations in the process of satellite image acquisition, the misclassification of the river side plants is likely to be improved by further development in the methodology. According to the feature extraction processes, the river side plant can be more similar to rice than the other land covers because it shares a unique time-series image pattern with rice paddy as they are sometimes flooded, and the texture became coarse as they grow. Therefore, creating an independent label for the river side plant by subdividing the class of others can minimize the confusion between them. At the same time, the process of adapting domain knowledge to deep learning applications requires more careful consideration, as broad interpretations of the adjacent time series could have contributed to further obscure the distinction between rice paddy and river side plant. Furthermore, since it is hard to consider every environmental or phenological difference in domain adaptation process, using confined training area could result in low performance at different sites. As a result, proper range of application area should be determined in consideration of the regional specificity of the training area and the extent to which the adapted domain knowledge could widen model's applicability.

B. Statistical Evaluation on City Level

Fig. 11 shows the results of linear regression between the detected rice paddy area and city-level statistics provided by Korean Statistics. All of the models had a relatively high correlation with the statistical data; however, the difference in the trend of the linear equation was identified according to the learning material. The trend of the linear equation from the models using PLM was well matched with the statistics, whereas the models using DALM tended to overestimate the rice paddy area, and models using SSCLM tended to underestimate it. The R^2 value was highest for the models using DALM, followed by the models using PLM, and the models using SSCLM.

Considering that all of the application sets have improved classification performance in most of the sites, data augmentation was effective in increasing recall, as the trend line indicates overestimation compared with the baseline application set. Meanwhile, semisupervised classification was effective in increasing specificity, which is the recall of the negative class, as the trend line indicates underestimation. Compared with the applications on learning materials, domain adaptation in deep learning architecture had a minimal impact on the trend line and R^2. On the one hand, both of the deep learning architectures used in this article seem to be complex enough to extract sufficiently abstract features from the Sentinel-1 time-series data. Therefore, other types of domain adaptation strategies or applications on more complex data with

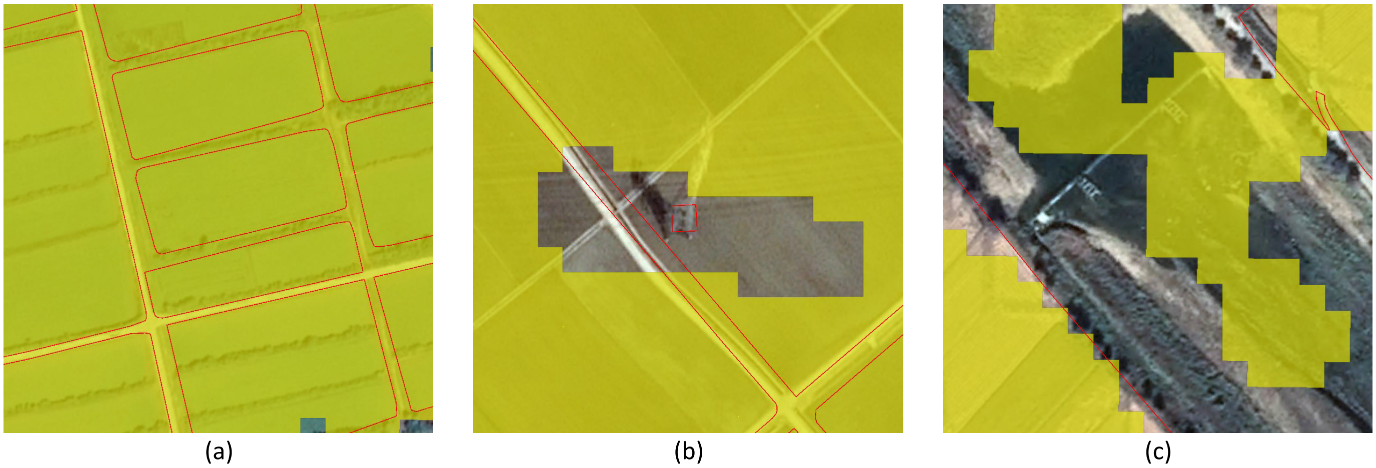

Fig. 10. Major factors causing misclassification. (a) Small objects. (b) Artificial structures. (c) River side plants.

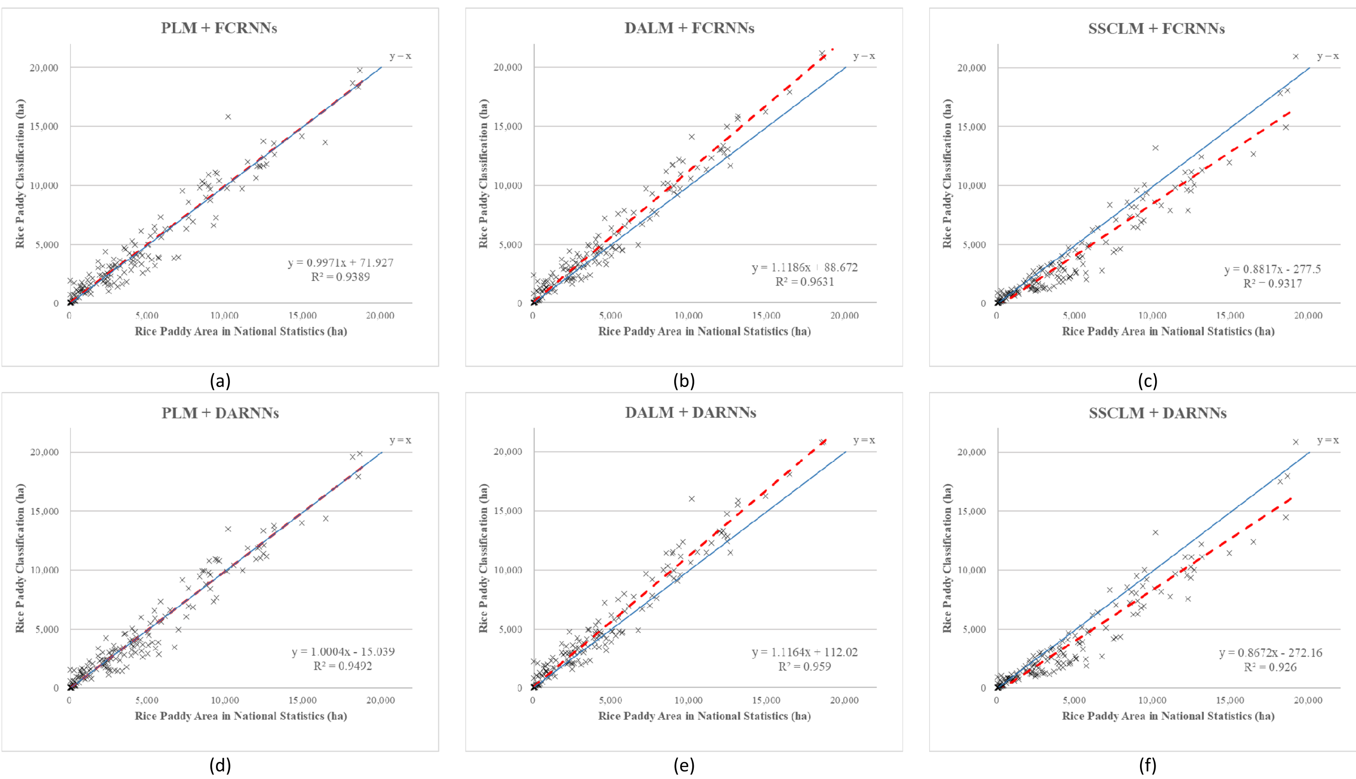

Fig. 11. Linear regression for rice paddy area between national statistics and model classification. (a) PLM + FCRNNs. (b) DALM + FCRNNs. (c) SSCLM + FCRNNs. (d) PLM + DARNNs. (e) DALM + DARNNs. (f) SSCLM + DARNNs.

higher resolution should be examined for more clarification on the effect of domain-adapted architecture. On the other hand, considering that the domain-adapted architecture almost maintained the trend line with somewhat increasing accuracy in pixel-based evaluation, it has the effect of both increasing recall and specificity.

Meanwhile, it should be noted that even though the slope can be an indicator for describing relative over- or underestimation, comparing pixel-based classification and statistical data on the same line is difficult. Because of the differences in the rice paddy estimation method between the land cover map and city-level statistics, judging the quality of classification performance by slope is challenging. The existence of any bias based on the extent of the inclusion of paddy levee into the rice paddy should be verified.

Therefore, focusing on R^2 rather than slope to estimate the performance, DALM which was found to be the best performing learning material in the pixel-based evaluation, also showed remarkably high R^2 in the statistical evaluation, compared with the others. To fully utilize the result with high explanatory power, developing a slope-based constant calibration coefficient for converting pixel-based classification to the national standard of rice paddy estimation is recommended. In that case, the reduction in cost by substituting the field survey intensive statistics with a remote sensing model would be a benefit. Recently, Korean governmental agencies, such as the Korea Forest Service, Rural Development Administration, and Korea Aerospace Research Institute, have been planning to launch an agro-forestry satellite, which will provide high spatio-temporal resolution with 5-m resolution and 1–3 days revisit time, in 2023. Promoting the applicability of deep learning to remote sensing and developing a postprocessing technique will maximize the use of such newly launched satellites by producing or substituting national information with remote sensing data.

V. Conclusion

Deep learning is an emerging technology in the remote sensing field as a method for fully utilizing big data, which is generated by increasing the spatio-temporal resolution of satellite images. However, although the applicability of deep learning is experimentally verified in various studies, the relative insufficiency of labeled data in the remote sensing field is a significant factor that impairs the usability of deep learning. In this article, diverse deep learning applications, such as data augmentation, semi-supervised classification, and domain-adapted architecture, were examined to overcome the insufficiency of labeled data by integrating the domain knowledge of remote sensing and the classification target. As a result, it was found that each combination of those applications slightly or dramatically improved the classification performance in rice paddy detection. Among them, data augmentation considering the differences in rice phenology had the greatest effect on improving classification performance, and this improvement was confirmed in both pixel-based and statistical evaluation. Improving the nationwide paddy detection performance was made possible by simulating the condition of various planting periods from a confined rice-growing area. Semisupervised classification also improved the accuracy and Cohen's kappa value in overall evaluation plots, even though identifying explicit performance improvement in the statistical evaluation was difficult. Because of the uncertainty of exploiting unlabeled data, the application should be carefully adapted with sufficient verification processes to confirm its positive impact. The domain-adapted architecture had the least effect on performance compared with the other applications. Considering that the domain-adapted architecture clearly increased accuracy and kappa value when it was applied to PLM without other applications, the low effect on the other cases can partially come from the duplication of adapted domain knowledge in both the architecture and learning material. The combination of applications did not significantly increase the performance, but at least, it followed better performance among the combination, demonstrating that combination of diverse applications would be optimal when neither of them is committed to a practical task. All the examined applications above were focused on describing the overall data distribution of the classification target with a confined labeled area. Therefore, this method can be used to generalize classification algorithms and would be more meaningful when the classification target has high intraclass heterogeneity due to the use of high-resolution images and the study of a wide-ranging area with diverse environment. In this context, our future study will be conducted on the entire Korean peninsula including North Korea which shares similar agricultural pattern with South Korea with having latitudinal differences in environment. Since the spatial information is extremely limited, North Korea is expected to be an ideal testbed for the proposed applications to overcome limited labeling data.

Although the examined applications generally increased classification performance by overcoming the limitation of insufficient labeled data, they should be carefully used as they may increase obscurity in some particular cases by imitating or utilizing unlabeled data. In addition, even though an effort was made to perform evaluation in diverse environments with two different approaches, further examination on these applications in even more diverse classification targets with other satellite images, especially with more high-resolution data sets, should be performed. In addition, it is necessary to determine whether additional performance improvements or reduction occurs when different types of domain knowledge are adapted in combination. For example, it should be confirmed whether there are any negative aspects to combining different domain knowledge for each application method.

Appendix

See Table II.

References

[1] Y. Ma *et al.*, "Remote sensing big data computing: Challenges and opportunities," *Future Gener. Comput. Syst.*, vol. 51, pp. 47–60, Oct. 2015.

[2] M. Chi, A. Plaza, J. A. Benediktsson, Z. Sun, J. Shen, and Y. Zhu, "Big data for remote sensing: Challenges and opportunities," *Proc. IEEE*, vol. 104, no. 11, pp. 2207–2219, Nov. 2016.

[3] M. M. Najafabadi, F. Villanustre, T. M. Khoshgoftaar, N. Seliya, R. Wald, and E. Muharemagic, "Deep learning applications and challenges in big data analytics," *J. Big Data*, vol. 2, no. 1, pp. 1–21, Dec. 2015.

[4] C. Sun, A. Shrivastava, S. Singh, and A. Gupta, "Revisiting unreasonable effectiveness of data in deep learning era," in *Proc. IEEE Int. Conf. Comput. Vis. (ICCV)*, Oct. 2017, pp. 843–852.

[5] S. Jagannathan, "Real-time big data analytics architecture for remote sensing application," in *Proc. Int. Conf. Signal Process., Commun., Power Embedded Syst. (SCOPES)*, Oct. 2016, pp. 1912–1916.

[6] S. Y. Hong, S.-I. Na, K.-D. Lee, Y.-S. Kim, and S.-C. Baek, "A study on estimating rice yield in DPRK using MODIS NDVI and rainfall data," *Korean J. Remote Sens.*, vol. 31, no. 5, pp. 441–448, Oct. 2015.

[7] D. H. T. Minh *et al.*, "Deep recurrent neural networks for winter vegetation quality mapping via multitemporal SAR Sentinel-1," *IEEE Geosci. Remote Sens. Lett.*, vol. 15, no. 3, pp. 464–468, Mar. 2018.

[8] N. Kussul, M. Lavreniuk, S. Skakun, and A. Shelestov, "Deep learning classification of land cover and crop types using remote sensing data," *IEEE Geosci. Remote Sens. Lett.*, vol. 14, no. 5, pp. 778–782, May 2017.

[9] E. Ndikumana, D. H. T. Minh, N. Baghdadi, D. Courault, and L. Hossard, "Deep recurrent neural network for agricultural classification using multitemporal SAR Sentinel-1 for Camargue, France," *Remote Sens.*, vol. 10, no. 8, p. 1217, 2018.

[10] D. B. Nguyen and W. Wagner, "European rice cropland mapping with Sentinel-1 data: The mediterranean region case study," *Water*, vol. 9, no. 6, p. 392, 2017.

[11] N. Muralidhar, M. R. Islam, M. Marwah, A. Karpatne, and N. Ramakrishnan, "Incorporating prior domain knowledge into deep neural networks," in *Proc. IEEE Int. Conf. Big Data (Big Data)*, Dec. 2018, pp. 36–45.

[12] C.-H. Lim, Y. S. Kim, M. Won, S. J. Kim, and W.-K. Lee, "Can satellite-based data substitute for surveyed data to predict the spatial probability of forest fire? A geostatistical approach to forest fire in the republic of Korea," *Geomatics, Natural Hazards Risk*, vol. 10, no. 1, pp. 719–739, Jan. 2019.

[13] Y. Inoue, E. Sakaiya, and C. Wang, "Capability of C-band backscattering coefficients from high-resolution satellite SAR sensors to assess biophysical variables in paddy rice," *Remote Sens. Environ.*, vol. 140, pp. 257–266, Jan. 2014.

[14] J. M. Lopez-Sanchez, F. Vicente-Guijalba, J. D. Ballester-Berman, and S. R. Cloude, "Polarimetric response of rice fields at C-band: Analysis and phenology retrieval," *IEEE Trans. Geosci. Remote Sens.*, vol. 52, no. 5, pp. 2977–2993, May 2014.

[15] L. R. Mansaray, D. Zhang, Z. Zhou, and J. Huang, "Evaluating the potential of temporal sentinel-1A data for paddy rice discrimination at local scales," *Remote Sens. Lett.*, vol. 8, no. 10, pp. 967–976, Oct. 2017.

[16] Ministry of Environment Korea. *Environmental Geographic Information Service: Land Cover Map*. Accessed: Jul. 22, 2019. [Online]. Available: https://egis.me.go.kr/intro/land.do

[17] D. Bargiel, "A new method for crop classification combining time series of radar images and crop phenology information," *Remote Sens. Environ.*, vol. 198, pp. 369–383, Sep. 2017.

[18] *Nong-Eob-Gyeong-Yeong-Gwan-Li-Gil-Jab-I 6: Ssal Gyeong-Yeong-Gwan-Li [A Guide for Agricultural Management 6: Rice Management]*, Rural Development Administration of South Korea, Wansan-gu, South Korea, EDEN Welfare Foundation EDEN House, 2016.

[19] P. W. Tse and D. P. Atherton, "Prediction of machine deterioration using vibration based fault trends and recurrent neural networks," *J. Vibrat. Acoust.*, vol. 121, no. 3, pp. 355–362, Jul. 1999.

[20] Y. Bengio, A. Courville, and P. Vincent, "Representation learning: A review and new perspectives," *IEEE Trans. Pattern Anal. Mach. Intell.*, vol. 35, no. 8, pp. 1798–1828, Aug. 2013.

[21] S. Ioffe and C. Szegedy, "Batch normalization: Accelerating deep network training by reducing internal covariate shift," 2015, *arXiv:1502.03167*. [Online]. Available: http://arxiv.org/abs/1502.03167

[22] A. Kamilaris and F. X. Prenafeta-Boldú, "Deep learning in agriculture: A survey," *Comput. Electron. Agricult.*, vol. 147, pp. 70–90, Apr. 2018.

[23] Rural Development Administration Korea. (2017). *Byu Gi-Gae Monaegi [Machinery Rice Transplanting]*. Accessed: Jul. 22 2019. [Online]. Available: http://www.nongsaro.go.kr/portal/ps/psv/psvr/psvre/curationDtl.ps?menuId=PS03352&srchCurationNo=1025&pageUnit=10&pageIndex=1&sEraInfo=&sSrchAll=&sKidofcomdtySeCode=&srchStr= &srchAll=Y

[24] J. M. Lopez-Sanchez, J. D. Ballester-Berman, and I. Hajnsek, "Rice monitoring in Spain by means of time series of terraSAR-X dual-pol images," in *Proc. Int. Workshop Appl. Polarimetry Polarimetric Interferometry (Pol-InSAR)*, vol. 668, Jan. 2009, pp. 26–30.

[25] T. Blaschke, "Object based image analysis for remote sensing," *ISPRS J. Photogramm. Remote Sens.*, vol. 65, no. 1, pp. 2–16, Jan. 2010.

[26] L. Drăguţ, D. Tiede, and S. R. Levick, "ESP: A tool to estimate scale parameter for multiresolution image segmentation of remotely sensed data," *Int. J. Geographical Inf. Sci.*, vol. 24, no. 6, pp. 859–871, Apr. 2010.

[27] S. Park, J. Im, S. Park, C. Yoo, H. Han, and J. Rhee, "Classification and mapping of paddy rice by combining landsat and SAR time series data," *Remote Sens.*, vol. 10, no. 3, p. 447, 2018.

[28] O. Abdel-Hamid, L. Deng, and D. Yu, "Exploring convolutional neural network structures and optimization techniques for speech recognition," in *Proc. Annu. Conf. Int. Speech Commun. Assoc.*, Aug. 2013, pp. 3366–3370.

[29] R. Liu, G. Meng, B. Yang, C. Sun, and X. Chen, "Dislocated time series convolutional neural architecture: An intelligent fault diagnosis approach for electric machine," *IEEE Trans. Ind. Informat.*, vol. 13, no. 3, pp. 1310–1320, Jun. 2017.

[30] Statistics Korea. (2018). *Crop Production Survey*. Accessed: Jul. 22, 2019. [Online]. Available: http://kosis.kr/eng/statisticsList/statisticsListIndex.do?menuId=M_01_01&vwcd=MT_ETITLE&parmTabId=M_01_01&statId=1967001&themaId=#SelectStatsBoxDiv

[31] Statistics Korea. (2018). *Statistical Survey Outlines*. Accessed: Jul. 22, 2019. [Online]. Available: http://www.narastat.kr/metasvc/svc/SvcMetaDcDtaPopup.do?confmNo=114004

[32] R. K. Srivastava, K. Greff, and J. Schmidhuber, "Training very deep networks," in *Proc. Adv. Neural Inf. Process. Syst.*, 2015, pp. 2377–2385.

[33] Q. Yu, P. Gong, N. Clinton, G. Biging, M. Kelly, and D. Schirokauer, "Object-based detailed vegetation classification with airborne high spatial resolution remote sensing imagery," *Photogramm. Eng. Remote Sens.*, vol. 72, no. 7, pp. 799–811, Jul. 2006.

[34] L. Zhang, K. Jia, X. Li, Q. Yuan, and X. Zhao, "Multi-scale segmentation approach for object-based land-cover classification using high-resolution imagery," *Remote Sens. Lett.*, vol. 5, no. 1, pp. 73–82, Jan. 2014.

[35] J. L. Riera, J. J. Magnuson, J. R. V. Castle, and M. D. MacKenzie, "Analysis of large-scale spatial heterogeneity in vegetation indices among North American landscapes," *Ecosystems*, vol. 1, no. 3, pp. 268–282, May 1998.

[36] A. Moumtzidou, M. Bakratsas, S. Andreadis, G. Ilias, V. Stefanos, and K. Ioannis, "Road passability estimation using deep neural networks and satellite image patches," in *Proc. BiDS*, Munich, Germany, 2019, pp. 1–4, doi: 10.2760/848593.

[37] Y. Wang and S. Chen, "Safety-aware semi-supervised classification," *IEEE Trans. Neural Netw. Learn. Syst.*, vol. 24, no. 11, pp. 1763–1772, Nov. 2013.

Hyun-Woo Jo received the B.S. degree in environmental science and ecological engineering from Korea University, Seoul, South Korea, in 2018, where he is pursuing the M.S. and Ph.D. integrated degree in environmental planning and landscape architecture.

During his degree course, he is involved in the H2020-EOPEN Project (opEn interOperable Platform for unified access and analysis of Earth observatioN data) and a developed deep-learning-based rice paddy detection model, which is integrated on the platform. His research interests include processing remote sensing data with deep-learning techniques in the field of agroforestry and integrating data science concepts with field specific domain knowledge.

Sujong Lee received the B.S. degree in environmental science and ecological engineering from Korea University, Seoul, South Korea, in 2019, where he is pursuing the M.S. and Ph.D. integrated degree in environmental planning and landscape architecture.

His research interests include remote-sensed land cover classification based on statistical density estimation, spectral vegetation indices, and machine learning.

Eunbeen Park received the B.S. degree in geology from Kangwon National University, Chuncheon, South Korea, in 2017. She is currently pursuing the M.S. and Ph.D. integrated degree in environmental planning and landscape architecture from Korea University, Seoul, South Korea.

During her degree course, she is involved in UN ESCAP project for drought monitoring and early warning through the Regional Drought Mechanism. Her research interest includes monitoring land change detection using remote-sensed data and environmental nexus based on modeling.

Chul-Hee Lim received the M.S. degree in environmental policy and management from Sejong University, Seoul, South Korea, in 2013, and the Ph.D. degree in water–food–ecosystem nexus to climate change from the Department of Environmental Science and Ecological Engineering, Korea University, Seoul, in 2017.

He is a Research Professor with the Institute of Life Science and Natural Resources, and also with the Environmental GIS/RS Center, Korea University, Seoul. He is involved in research on climate change impact–adaptation, environmental change impact (such as deforestation) using process-based and machine learning models, spatial modeling of agriculture–water–ecosystem–disaster, and their interactions, environmental policy and planning, and other various environmental issues (air pollution, ecosystem services, and desertification).

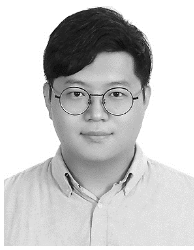

Cholho Song received the Ph.D. degrees in environmental planning and landscape architecture from Korea University, Seoul, South Korea.

He was one of the participants of the program between Korea National Research Foundation (NRF) and Deutscher Akademischer Austauschdienst (DAAD) program and the International Institute for Applied Systems Analysis (IIASA) 2017 Young Scientists Summer Program (YSSP). He focused on developing assessment framework of ecosystem services and process-based ecosystem modeling using geographic information systems and remote sensing in the forest sector. He is currently a Research Professor with the Ojeong Eco-Resilience Institute (OJERI), Korea University. His research interests are ecosystem services for land accounts, land changes monitoring, and environmental planning using geospatial models and integrated assessment systems.

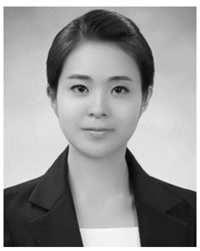

Halim Lee received the B.S. degree in business administration and English language and literature from Ewha Womans University, Seoul, South Korea, in February 2015. She is currently pursuing the M.S degree in environmental planning and landscape architecture from Korea University, Seoul.

During her master's study, she is involved in H2020-EOPEN Project and UN ESCAP Project for enhancing regional cooperation and capacity of geospatial information systems (GIS) for disaster risk reduction (DRR) in Central Asia.

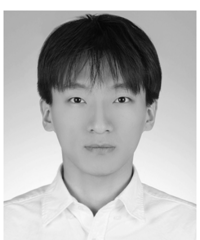

Youngjin Ko received the B.S. degree in forest science from Chonnam National University, Gwangju, South Korea, in 2016. He is pursuing the M.S. and Ph.D. integrated degree in environmental planning and landscape architecture with Korea University, Seoul, South Korea.

His research interest includes monitoring water balance in forestry by using remote sensing data. He is also devoted to developing strategies for using harvested wood product to achieve greenhouse gas reduction and climate change mitigation in a concept of BECCS.

Sungeun Cha received the B.S. degree in computer science from Korea University, Seoul, South Korea, in 2015, where he is pursuing the M.S. and Ph.D. integrated degree in environmental planning and landscape architecture.

During his Ph.D. course, he is focusing on remote sensing based modeling for forest management, carbon stock change due to climate change, and disaster risk reduction (DRR). He also participated in the International Institute for Applied Systems Analysis (IIASA) 2018 Young Scientists Summer Program (YSSP), Laxenburg, Austria, where he studied the Convolutional Neural Networks (CNNs) for estimating forest growing stock volume of the entire forests in South Korea.

Hoonjoo Yoon is serving as the CEO of Sundosoft, Ltd., Seoul, South Korea. He developed a proven innovation framework to address public sector problems that could be used among stakeholders while working with various experts on the GIS platform. He was awarded the Prime Minister's Award for exporting its environmental impact assessment system and waste management platform to Vietnam.

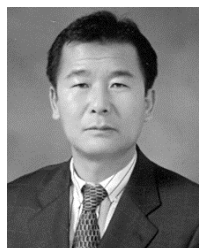

Woo-Kyun Lee received the B.S. degree and the M.S. degree in forestry from Korea University, Seoul, South Korea, in 1987 and 1989, respectively, and the Ph.D. degree in agriculture from Georg-August-Universität Göttingen, Göttingen, Germany, in 1993.

He is a Professor with the Department of Environment Science and Ecological Engineering, the Director of the Environmental GIS/RS Center with Korea University. Academically, he is President of the Korean Society of Remote Sensing (KSRS) and the Korean National Committee for International Institute of Applied System Analysis (IIASA). Internationally, he has served as the Director of SDSN Korea, Mid-Latitude Region Network (MLRN), Scientific Steering Committee of GCP-Korea Office. His research has been focused on the region of the Mid-Latitude Ecotone, including the Korean Peninsula, North-Eastern Asia, and Central Asian countries, where extreme climate conditions are increasing water and food problems. His current work focuses on development of indicators for sustainable development goals (SDGs), disaster risk reduction (DRR), and climate change considering environmental and socioeconomic conditions in MLR. He has provided suggestions on how to enhance adaptive capacity or resilience through environmental infrastructure and socioeconomic policies for adapting climate change, reducing disaster risk, and achieving SDGs.